For this problem, the domain was discretized by using 51 equally spaced grid points in the streamwise direction (x direction) and 125 nonequally spaced grid points in the direction normal to the plate (y direction). In the y direction, grid points were clustered towards the plate (where $y = 0$), and grid spacings varied from 6×10^{-7} m at $y = 0$ (corresponding to $y^+ = \rho u_\tau y/\mu = 0.2$) to 0.025 m at $y = 0.25$ m which resulted in 11 grid points in the linear sublayer ($0 \leq y^+ \leq 3$), 24 grid points in the buffer layer ($3 < y^+ \leq 40$), and 75 grid point in the fully turbulent region.

The equations used to model the turbulent boundary-layer flow are the ensemble-averaged conservation equations of mass, momentum (thin-layer Navier-Stokes), and total energy valid for a calorically and thermally perfect gas. The ensemble-averaged conservation equations were closed by the k-ε model of Chen and Patel which was described in the previous section. In this study, the turbulence model lagged behind the conservation equations of mass, momentum, and total energy by one timestep in the solution procedure. Solutions to the conservation equations were obtained by using the F3D code developed by Steger et al.[10] Solutions to the turbulence model were obtained by using the algorithm described in the previous section; the code which embodies this algorithm will be referred to as RAAKE.

Solutions were first obtained to examine the robustness of the algorithm developed by running RAAKE with the diffusion terms treated explicitly and then implicitly. When the diffusion terms were treated explicitly, numerical experiments indicated that for the current test problem stable numerical solutions can only be obtained if the time-step size is less than about 1×10^{-8} s which is comparable to the maximum timestep size permitted by the explicit stability criterion from linearized analysis (i.e., $\alpha\Delta t/\Delta y^2 \leq 1/2$, $\alpha = (\mu + \mu_t/\sigma_k)/\rho$; see Eq. (7) and set $a = 0$ because convection is negligible in that direction and set $b = \alpha\Delta t/\Delta y^2$). When the diffusion terms were treated implicitly, numerical experiments indicated that stable numerical solutions can be obtained with a time-step size as large as 1×10^{-4} s which is also the largest timestep size that can be used by the F3D code for the test problem.

With the robustness of the algorithm established, solutions were obtained to assess its accuracy. This was achieved by using the F3D code with RAAKE in which the diffusion terms were treated implicitly. The time-step size used was 1×10^{-5} s. Solutions were obtained for $k^+ = k/(u_\tau)^2$, $\varepsilon^+ = \mu_w \varepsilon/\rho_w U_z^4$, and $u^+ = u/u_\tau$ as a function of $y^+ = \rho u_\tau y/\mu$, where $u_\tau = \sqrt{\tau_w \rho_w}$ is the friction velocity, and the subscript w denotes $y = 0$. The solutions obtained for k^+ and ε^+ are shown in Fig. 1, and they compare well with the known behavior of these quantities[11] (i.e., they fall within the band of available experimental data). The solution obtained for u^+ as a function of y^+ is not shown, but is in excellent agreement (less than 0.05% difference) with the solution obtained by using the Baldwin-Lomax model[12] which is known to provide the correct solution for the current test problem.

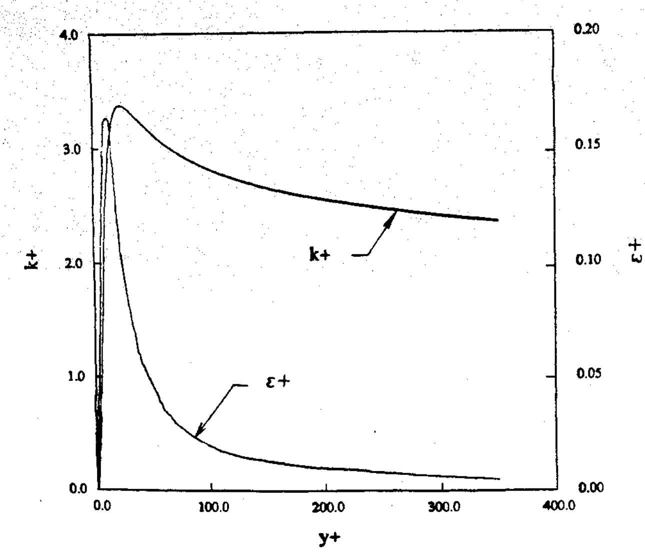

Fig. 1 Solution obtained for k^+ and ε^+ as a function of y^+.

These numerical experiments indicate that the method presented in this study for treating diffusion terms implicitly for the LU algorithm is useful in improving robustness for problems where diffusion terms play an important role.

References

[1]Jameson, A., and Turkel, E., "Implicit Schemes and LU Decompositions," *Mathematics of Computations*, Vol. 37, No. 156, 1981, pp. 385–397.

[2]Steger, J. L., and Warming, R. F., "Flux Vector Splitting of the Inviscid Gasdynamics Equations with Application to Finite-Difference Methods," *Journal of Computational Physics*, Vol. 40, No. 2, 1981, pp. 263–293.

[3]Yoon, S., and Jameson, A., "Lower-Upper Symmetric-Gauss-Seidel Method for the Euler and Navier-Stokes Equations," *AIAA Jounal*, Vol. 26, No. 9, 1988, pp. 1025–1026.

[4]Shuen, J. S., and Yoon, S., "Numerical Study of Chemically Reacting Flows Using a Lower-Upper Symmetric Successive Overrelaxation Scheme," *AIAA Journal*, Vol. 27, No. 12, 1989, pp. 1752–1760.

[5]Yokota, J., "A Diagonally Inverted Lower-Upper Factored Implicit Multigrid Scheme for the Three-Dimensional Navier-Stokes Equations," *AIAA Journal*, Vol. 28, No. 9, 1990, pp. 1642–1649.

[6]Gatlin, B., and Whitfield, D. L., "An Implicit, Upwind, Finite-Volume Method for Solving the Three-Dimensional, Thin-Layer Navier-Stokes Equations," AIAA Paper 87-1149, June 1987.

[7]Chen, H. C., and Patel, V. C., "Near-Wall Turbulence Models for Complex Flows including Separation," *AIAA Journal*, Vol. 26, No. 6, 1988, pp. 641–648.

[8]Wolfshtein, M., "The Velocity and Temperature Distribution in One-Dimensional Flow with Turbulence Augmentation and Pressure Gradient," *International Journal of Heat and Mass Transfer*, Vol. 12, March 1969, pp. 301–318.

[9]Shih, T. I-P., and Chyu, W. J., "Approximate-Factorization with Source Terms," *AIAA Journal*, Vol. 29, No. 10, 1991, pp. 1759–1760.

[10]Steger, J. L., Ying, S. X., and Schiff, L. B., "A Partially Flux-Split Algorithm for Numerical Simulation of Compressible Inviscid and Viscous Flow," Proceedings of the Workshop on Computational Fluid Dynamics, Institute of Nonlinear Sciences, University of California, Davis, CA, 1986.

[11]Patel, V. C., Rodi, W., and Scheuerer, G., "Turbulence Models for Near-Wall and Low Reynolds Number Flows: A Review," *AIAA Journal*, Vol. 23, No. 9, 1985, pp. 1308–1319.

[12]Baldwin, B., and Lomax, H., "Thin Layer Approximation and Algebraic Model for Separated Turbulent Flows," AIAA Paper 78-257, Jan. 1978.

Eigenvalue Sensitivity with Respect to Location of Internal Stiffness and Mass Attachments

B. P. Wang*

University of Texas at Arlington, Arlington, Texas 76019

Introduction

In recent years, sensitivity analysis has attracted great attention in the research community.[1–4] Both static responses and eigenvalue sensitivity with respect to size and shape design variables have been treated. Eigenvalue sensitivity considering shape variables is less developed. Recently, eigenvalue sensitivity for support locations have been reported.[5,6] Specifically, Hon and Chuang[5] applied a material derivative concept in continuum mechanics to derive eigenvalue sensitivity with respect to beam support locations. This result shows that the eigenvalue sensitivity

Received Jan. 31, 1992; presented as Paper 92-2513 at the AIAA/ASME/ASCE/AHS/ASC 33rd Structures, Structural Dynamics, and Materials Conference, Dallas, TX, April 13–15, 1992; revision received Sept. 17, 1992; accepted for publication Sept. 17, 1992.

*Professor, Department of Mechanical and Aerospace Engineering. Member AIAA.

is related to the slope of the corresponding mode shape of the beam at the support and the support reaction. Over a decade earlier, Rozvany and Mroz[6] observed that the optimum hinge location for a column is where the reaction vanishes. Even though eigenvalue (for buckling for this case) sensitivity was not mentioned explicitly, their conclusion agrees with the sensitivity formula presented by Hon and Chuang.[5]

In this Note, formulas for eigenvalue sensitivity with respect to location of discrete in-span occurrence for structure members are derived using a normal mode method. The structural members treated in this Note include bars and plates and in-span occurrences which include concentrated mass and inertia, rigid supports, elastic supports, and appended spring-mass systems. Using the approach described in the next section, closed-form formulas are derived based on the classical normal mode method. It turns out that the results are all of the same form with different interpretations of the terms for specific cases.

General Approaches and Main Results

The sensitivity of eigenvalue with respect to support location has been derived using the concept of material derivatives.[5] In this Note, we choose a different approach. First, we use basic principles of structural mechanics and normal method to derive characteristics equations which include the location of an in-span occurrence as a parameter. Taking the derivative of this equation with respect to the in-span location yields, after some manipulations, the following general equation for computing the rth eigenvalue with respect to the in-span locations.

$$\frac{\partial \lambda_r}{\partial z} = -\frac{2\theta F_a}{M_r} \tag{1}$$

where

$$\theta = \phi_r'(z) \tag{2}$$

Here, ϕ_r is the rth eigenfunction, M_r the generalized mass of mode r, z the location of in-span occurrence, and F_a a characteristic force which depends on the specific occurrence. Table 1 summarizes F_a for various occurrences. Detailed derivation of Eq. (1) is given in the next section.

Derivation of the General Results

Consider the system shown in Fig. 1a which hereafter will be referred to as system A. System A can be considered as system B of Fig. 1b with a discrete in-span occurrence at z. By treating the occurrence as an external load, the response of system A can be computed using the eigensolutions of system B by classical normal mode method. The free vibration of system A can be considered as system B with a sinusoidal force $F_a e^{i\Omega t}$ applied at the location of in-span occurrence. The response of system B is

$$w(x, t) = W(x)e^{i\Omega t} \tag{3}$$

Table 1 Interpretation of F_a for various types of conditions

Occurrence	Equation for F_a	Interpretation
Rigid support	N/A	Modal reaction force
Elastic support		
Linear	$-k\,\phi_r(z)$	Spring force (positive when spring in compression)
Rotational	$-k_\theta\,\phi_r'(z)$	Spring torque
Concentrated		
Mass	$m\,\phi_r(z)\lambda_r$	Inertia force
Inertia	$J\phi_r'(z)\lambda_r$	Inertia torque
Appended spring-mass system	$-k[\phi_m - \phi_r(z)]$	Force in spring (positive for compression) ϕ_m = mode shape coefficient of the appended mass

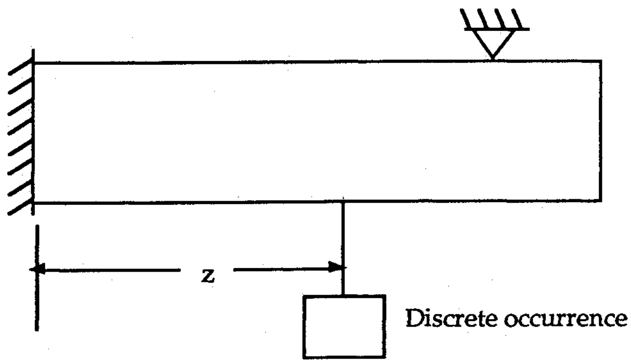

Fig. 1a System A: with discrete in-span occurrence.

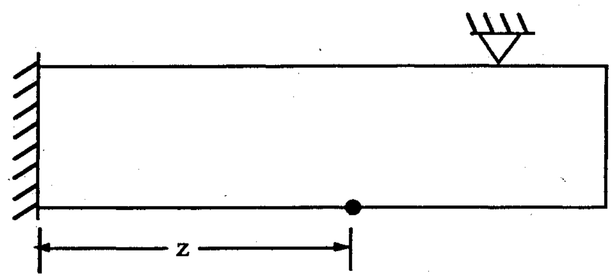

Fig. 1b System B: discrete occurrence removed.

where

$$W(x) = \sum_{i=1}^{\infty} \frac{\psi_i(x)\,\psi_i(z)\,F_a}{\omega_i^2 - \Omega^2} \tag{4}$$

and $\psi_i(x)$, ω_i^2 are the ith eigenfunction and the eigenvalue of system B. For a specific in-span occurrence, a frequency equation can be derived using the compatibility conditions between system B and the in-span occurrence. The solution Ω_j of this equation are the eigenvalues of system A.

Let us consider the case of an in-span support at z. In this case, the compatibility condition is

$$W(z) = 0 \tag{5}$$

which leads to the following frequency equation

$$\sum_{i=1}^{\infty} \frac{\psi_i^2(z)}{\omega_i^2 - \Omega^2} = 0 \tag{6}$$

Once an eigenvalue Ω_r^2 is computed from Eq. (6), the corresponding mode shape can be calculated by Eq. (4). Specifically, the rth mode of system A is

$$\phi_r(x) = \sum_{i=1}^{\infty} \frac{\psi_i(x)\,\psi_i(z)\,F_a}{\omega_i^2 - \Omega_r^2} \tag{7}$$

The eigenvalue sensitivity $(\partial\Omega_r^2/\partial z)$ can be derived by taking the derivative of Eq. (6) with respect to z. This leads to

$$\frac{\partial \Omega_r^2}{\partial z} = \left[-\sum_{i=1}^{\infty} \frac{2\psi_i(z)\,\psi_{i'z}'}{\omega_i^2 - \Omega_r^2} F_a \Bigg/ \sum_{i=1}^{\infty} \frac{\psi_i^2(z)\,F_a}{(\omega_i^2 - \Omega_r^2)^2} \right] \tag{8}$$

Now it remains to express Eq. (8) in terms of the eigensolution of system A. From Eq. (7)

$$\frac{\partial \phi_r}{\partial x} = \sum_{i=1}^{\infty} \left[\left(\frac{\partial \psi_i}{\partial x}\right) \psi_i(z)\,F_a \Big/ (\omega_i^2 - \Omega_r^2) \right] \tag{9}$$

or

$$\left.\frac{\partial \phi_r}{\partial x}\right|_{x=z} = \sum_{i=1}^{\infty} \frac{\psi_i'(z)\,\psi_i(z)\,F_a}{\omega_i^2 - \Omega_r^2} \tag{10}$$

where

$$\psi_i'(z) = \frac{\psi_i(z)}{\partial z} \tag{11}$$

The generalized mass of the rth mode of system A is

$$M_r = \int_0^{\ell} \phi_r^2(x)\,\mathrm{d}x \tag{12}$$

By using the definition of $\phi_r(x)$ of Eq. (7) and the orthonormal property of the eigenfunctions $\psi_i(x)$, the integration of Eq. (12) leads to

$$M_r = \sum \frac{\psi_i^2(z)}{(\omega_i^2 - \Omega_r^2)} F_a^2 \tag{13}$$

Using Eqs. (10) and (13), Eq. (8) yields the general results

$$\frac{\partial \Omega^2}{\partial z} = \frac{-2\partial \phi_r'(z)\,F_a}{M_r} \tag{14}$$

where

$$\phi_r'(z) = \left.\frac{\partial \phi_r}{\partial x}\right|_{x=z}$$

Examples

Two numerical examples are included in this section to demonstrate the use of Eq. (1) for eigenvalue sensitivity analysis.

Example 1: Rod with Discrete Mass and Spring Support

Consider a uniform rod of length 100 in. with cross-sectional area of 10 in.^{2}. A concentrated mass of 0.1 lb-s^2/in. and a spring

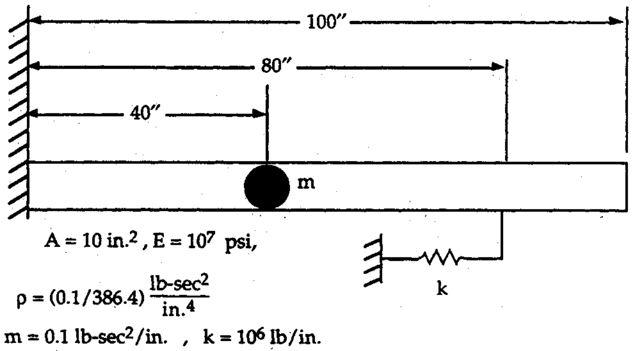

Fig. 2 Rod with in-span mass and spring: A = 10 in.^{2}, E = 10^7 psi, ρ = (0.1/386.4) (lb-s^2/in.^{4}), m = 0.1 lb/s^2/in., and k = 10^6 lb/in.

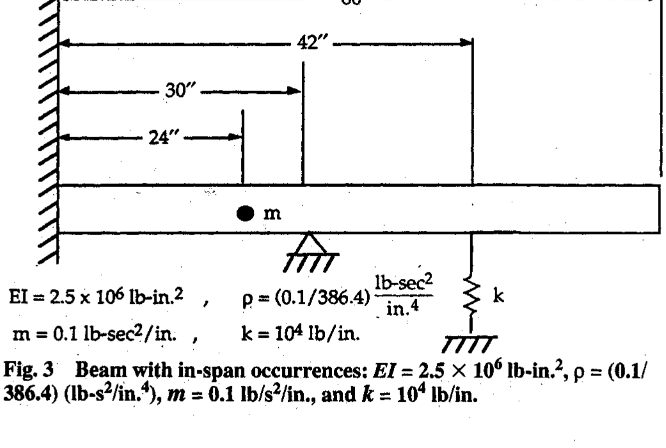

Fig. 3 Beam with in-span occurrences: EI = 2.5 × 10^6 lb-in.^{2}, ρ = (0.1/386.4) (lb-s^2/in.^{4}), m = 0.1 lb/s^2/in., and k = 10^4 lb/in.

Table 2 Eigenvalue sensitivity with respect to location of mass or spring for axial vibration

Case	OFD[a]	Sensitivity formula: Forward difference[b]	Sensitivity formula: Central difference[b]
Mass location, $\Delta z = 0.01$	−106,640	−53,960	−105,970
Spring location, $\Delta z = 0.001$	9,537	35,289	9,540

[a]Overall finite difference, see Eq. (17). [b]For computing ϕ_r' in Eq. (1).

Table 3 Eigenvalue sensitivity for beam with in-span occurrences

Case	OFD, (rad/s)^2/in.	Sensitivity formula, (rad/s)^2/in.
Mass location	246.5	246.5
Support location	−1733.4	−1734.4
Spring location	17,660	17,660

with stiffness 10^6 lb/in. are located at 40 in. and 80 in. from the fixed end, respectively; see Fig. 2. The equations for eigensolution sensitivity can be obtained from Table 1. They are for discrete mass:

$$\frac{\partial \lambda_r}{\partial z} = -2m\phi_r(40)\,\lambda_r\phi_r'(40) \tag{15}$$

for discrete spring:

$$\frac{\partial \lambda_r}{\partial z} = 2k\phi_r(40)\,\phi_r'(40) \tag{16}$$

Note that in Eqs. (15) and (16), the mode shape is assumed to be normalized to unit modal mass. The eigensolutions are obtained by finite element method (FEM) by dividing the system uniformly into 10 elements. Since for axial vibration via FEM the derivative of eigensolution at a grid point is not available, the term $\phi_r'(40)$ in Eq. (16) needs to be evaluated by finite difference. Both forward and central difference methods were used and the results are summarized in Table 2. Also shown in Table 2 is eigenvalue sensitivity evaluated by overall central finite difference (OFD) or

$$\frac{\partial \lambda_r}{\partial z} \approx \frac{\lambda_r(\Delta z) - \lambda_r(-\Delta z)}{2\Delta z} \tag{17}$$

It should be noted that the use of central difference to approximate $\phi_1'(40)$ yields good sensitivity data as compared with the results of OFD, whereas $\phi_1'(40)$ approximated by forward difference yields poor results.

Example 2: Beam with Discrete Mass, Spring, and In-Span Support

For the beam shown in Fig. 3, it is desired to find the sensitivity with respect to location of the in-span occurrences. From Eq. (1) and Table 1, the sensitivity with respect to location of mass, support, and discrete spring are given by the following formulas, respectively:

$$\frac{\partial \lambda_1}{\partial z} = -2m\phi_1(24)\,\phi_1'(24)\,\lambda_1 \tag{18}$$

$$\frac{\partial \lambda_1}{\partial z} = -2\phi_1'(30)\,F_a \tag{19}$$

$$\frac{\partial \lambda_1}{\partial z} = 2k\phi_1(42)\,\phi_1'(42) \tag{20}$$

The required eigensolution in the preceding equations are computed by finite element method using a 10-element model and the modes are normalized to unit model mass. The results are summarized in Table 3 along with those computed by overall finite difference with $\Delta z = 0.001$. The results agree with one another very well.

Concluding Remarks

Exact formulas for computing eigenvalue sensitivity with respect to location of in-span occurrence have been derived in this Note based on normal mode method. The results showed that for in-span occurrence with a single interface force, the eigenvalue sensitivity depends on the slope of eigenfunction as well as a force term which depends on the specific occurrence.

These formulas depend only on the eigensolutions and can be evaluated at almost no additional cost. For a specific problem, the eigenvalue sensitivity formula can be used qualitatively to determine the effect of moving one of the discrete occurrences. The quantitative data can be used to find locations of in-span occurrences to maximize the fundamental eigenvalue of a structure member.

References

[1]Adelman, H. M., and Haftka, R. T. (eds.), *Sensitivity Analysis in Engineering,* NASA CP 2457, NASA Langley Research Center, Hampton, VA, 1986.

[2]Adelman, H. M., and Haftka, R. T., "Sensitivity Analysis of Discrete Structural Systems," *AIAA Journal,* Vol. 24, No. 5, 1986, pp. 823–832.

[3]Huang, E. J., Choi, K. K., and Komkov, V., *Design Sensitivity Analysis of Structural Systems,* Academic Press, New York, 1986.

[4]Arora, J. S., and Huang, E. J, "Methods of Design Sensitivity Analysis in Structural Optimization," *AIAA Journal,* Vol. 17, No. 9, 1979, pp. 970–974.

[5]Hou, J. W., and Chuang, C. H., "Design Sensitivity Analysis and Optimization of Vibrating Beams with Variable Support Locations," *16th Automation Conference, ASME Transactions,* Chicago, IL, Sept. 1990; also, *Journal of Mechanisms, Transmissions, and Automation in Design* (to be published).

[6]Rozvany, G. I. N, and Mroz, Z., "Column Design: Optimization of Support Conditions and Segmentation," *Mechanics of Structures and Machines,* Vol. 5, No. 3, 1977, pp. 279–290.

Errata

Review of *Computational Methods in Hypersonic Aerodynamics*

G. V. Candler
University of Minnesota,
Minneapolis, Minnesota 55455

[AIAA Journal 31(2), p. 410 (1993)]

THE University of Minnesota was inadvertently printed as the University of Minneapolis. We regret this error.